Biochemical and Biophysical Research Communications 446 (2014) 921–926

Contents lists available at ScienceDirect

Biochemical and Biophysical Research Communications

journal homepage: www.elsevier.com/locate/ybbrc

Structural analysis of a putative SAM-dependent methyltransferase, YtqB, from *Bacillus subtilis* ☆

Sun Cheol Park [a], Wan Seok Song [a], Sung-il Yoon [a,b,*]

[a] Department of Systems Immunology, College of Biomedical Science, Kangwon National University, Chuncheon 200-701, Republic of Korea
[b] Institute of Bioscience and Biotechnology, Kangwon National University, Chuncheon 200-701, Republic of Korea

ARTICLE INFO

Article history:
Received 3 March 2014
Available online 14 March 2014

Keywords:
Bacillus subtilis
YtqB
Methyltransferase
S-adenosyl-L-methionine
Crystal structure

ABSTRACT

S-adenosyl-L-methionine (SAM)-dependent methyltransferases (MTases) methylate diverse biological molecules using a SAM cofactor. The *ytqB* gene of *Bacillus subtilis* encodes a putative MTase and its biological function has never been characterized. To reveal the structural features and the cofactor binding mode of YtqB, we have determined the crystal structures of YtqB alone and in complex with its cofactor, SAM, at 1.9 Å and 2.2 Å resolutions, respectively. YtqB folds into a β-sheet sandwiched by two α-helical layers, and assembles into a dimeric form. Each YtqB monomer contains one SAM binding site, which shapes SAM into a slightly curved conformation and exposes the reactive methyl group of SAM potentially to a substrate. Our comparative structural analysis of YtqB and its homologues indicates that YtqB is a SAM-dependent class I MTase, and provides insights into the substrate binding site of YtqB.

1. Introduction

S-adenosyl-L-methionine (SAM)-dependent methyltransferases (MTases) transfer a methyl group from a SAM cofactor to various types of acceptor molecules, including small chemicals and protein or nucleic acid macromolecules, yielding methylated products with S-adenosyl-L-homocysteine as a by-product [1]. MTases mediate a wide variety of cellular processes, such as cell signaling, metabolite synthesis, and gene regulation, in nearly all living organisms [2,3]. MTases can be grouped into five main classes (I–V), each of which contains a structurally distinct MTase fold although they catalyze the same methylation reaction [4]. Class I is the largest group of MTases and its members possess the canonical Rossmann-like fold as an MTase core structure. The Rossmann-like fold of class I MTases generally consists of seven β-strands flanked by two layers of α-helices to form the αβα sandwich, although some class I MTases deviate from the conserved topology of the core structure through omission of one or two β-strands or changes in β-strand organization [5].

Class I MTases exhibit common but distinct features in SAM and substrate binding. SAM binds to the spatially equivalent pocket at one end of the Rossmann-like domain, in part through conserved interactions with an acidic residue and the GxGxG or GxG motif [6,7]. However, each subgroup of class I MTases specifically interacts with SAM via different types of residues to properly orient the reactive methyl group of the SAM molecule toward a cognate methyl acceptor [5]. Although all class I MTases catalyze the methylation reaction via S_N2-like nucleophilic substitution, each MTase exerts a unique biological function that is determined by substrate specificity [1,2]. The substrates of the class I family have been reported to be highly variable and can range from small chemicals to macromolecules, including proteins, RNAs, and DNAs. Such substrate selectivity is provided by the structural features of the MTase, such as additional domains, the N-terminal appendage, and the active site cap [8–11]. Thus, to define the catalytic mechanism of MTases, structural studies on each MTase in complex with SAM and its substrate are required.

Bacillus subtilis is one of the most well-characterized Gram-positive bacteria that belong to phylum of Firmicutes, and it expresses a putative MTase, YtqB, with an as-yet uncharacterized biological function. YtqB contains 194 residues and is one of the shortest MTases. YtqB orthologs are found in diverse bacterial species from Firmicutes and Chlamydiae as well as some Proteobacteria. Here, we provide structural evidence that YtqB exhibits the canonical topology of class I MTases and is dimeric with one β-sheet sandwiched by α-helices. Moreover, the crystal structure of YtqB in complex with SAM revealed a cofactor binding mode that is conserved but unique compared to those of other types of class I MTases. Finally, our structural and sequence

☆ The atomic coordinates and structure factors for YtqB (PDB ID 4PON) and its complex with SAM (PDB ID 4POO) have been deposited in the Protein Data Bank, www.pdb.org.

* Corresponding author. Address: 1 Kangwondaehak-gil, Biomedical Science building A-204, Chuncheon 200-701, Republic of Korea. Fax: +82 33 250 8380.
E-mail address: sungil@kangwon.ac.kr (S.-i. Yoon).

http://dx.doi.org/10.1016/j.bbrc.2014.03.026
0006-291X/

analyses of a potential substrate binding site provide clues to the identity of the YtqB substrate.

2. Materials and methods

2.1. Construction of the YtqB expression vector and expression of the YtqB protein

The YtqB gene (residues 1–194) was amplified by PCR from the genomic DNAs of *B. subtilis* using primers that contain *Bam*HI or *Sal*I restriction enzyme sites. The resultant PCR products were cleaved using *Bam*HI or *Sal*I restriction enzymes, and ligated into a modified pET49b vector (pET49bm) containing the N-terminal His_6 tag and thrombin cleavage site [12,13]. The ligation products were transformed into *Escherichia coli* strain DH5α, and the sequence of the insert in the transformant was verified by DNA sequencing. YtqB expression vector DNA was transformed into *E. coli* strain BL21 (DE3), and YtqB expression was carried out in LB medium in the presence of 1 mM IPTG for ~17 h at 18 °C. The cells were harvested by centrifugation for purification of the YtqB protein.

2.2. Purification of the YtqB protein

The cells were sonicated in 50 mM Tris (pH 8.0), 200 mM NaCl, 5 mM β-mercaptoethanol (βME), and 1 mM PMSF, and the cell lysates were cleared by centrifugation. The YtqB protein was first purified by Ni–NTA affinity chromatography. The supernatant containing the YtqB protein was incubated with Ni–NTA resins (Qiagen) in the presence of 10 mM imidazole. The YtqB protein was eluted using 250 mM imidazole after a wash step with 10 mM imidazole. After dialysis and thrombin digestion, the YtqB protein was further purified by anion-exchange chromatography using a Mono Q 10/100 column (GE Healthcare) with a NaCl gradient (0.0–0.5 M). The resulting protein was concentrated to ~15 mg/ml for crystallization.

2.3. Crystallization of the YtqB protein and X-ray diffraction of YtqB crystals

The YtqB protein was crystallized by the sitting drop vapor diffusion method at 18 °C. YtqB crystals were obtained in a drop that contained 0.5 μl of ~15 mg/ml YtqB protein and 0.5 μl of 30–36% PEG200/5% PEG2000/0.1 M sodium cacodylate (pH 6.5) or 30–36% PEG200/5% PEG2000/0.1M Hepes (pH 7.0). To obtain SAM-bound YtqB ($YtqB^{SAM}$) crystals, YtqB crystals were soaked in 1 mM SAM/30–36% PEG200/5% PEG2000/0.1M Hepes (pH 7.0) for 6 h at room temperature. YtqB or $YtqB^{SAM}$ crystals were mounted and flash-frozen under the cryo-stream at −173 °C. X-ray diffraction was performed at beamline 7A of the Pohang Accelerator Laboratory (PAL). Diffraction data were processed using the HKL2000 package [14]. X-ray diffraction statistics are shown in Table 1.

2.4. Structure determination of YtqB

The YtqB structure was determined by molecular replacement with the *PHASER* program [15] using the structure coordinates of a putative MTase from *Clostridium thermocellum* (PDB ID 3EEY) as a search model. The YtqB structure was iteratively built and refined using the *COOT* and *REFMAC5* programs, respectively [16,17]. The structure refinement statistics are shown in Table 1.

Table 1
Crystallographic statistics of the YtqB structures.

	YtqB	$YtqB^{SAM}$
Data collection		
Space group	$P2_12_12_1$	$P2_12_12_1$
Cell parameters	a = 48.86 Å	a = 47.07 Å
	b = 76.57 Å	b = 77.66 Å
	c = 100.95 Å	c = 100.48 Å
Wavelength (Å)	0.97958	0.97939
Resolution (Å)	20.00–1.90	30.00–2.20
Highest resolution (Å)	1.97–1.90	2.28–2.20
No. observations	134,694	95,996
No. unique reflections	30,744	19,185
R_{merge} (%)[a]	7.8 (54.5)[b]	5.7 (47.2)[b]
I/sigma	31.7 (3.3)[b]	37.4 (2.9)[b]
Completeness (%)	99.3 (100.0)[b]	99.6 (98.4)[b]
Redundancy	4.4 (4.4)[b]	5.0 (4.7)[b]
Refinement		
Resolution (Å)	20.00–1.90	30.00–2.20
No. of reflections (total)	28,698	18,155
No. of reflections (test)	1526	982
R_{cryst} (%)[c]	20.0	22.0
R_{free} (%)[d]	23.6	26.0
Average B-value (Å^2)	35.8	52.2
No. protein atoms	2629	2595
No. of ligand atoms	0	54
No. water molecules	154	10
RMSD bonds (Å)	0.015	0.017
RMSD angles (°)	1.46	1.59
Ramachandran[e] (favored)	98.8%	98.5%
(outliers)	0%	0%

[a] $R_{merge} = \Sigma_{hkl}\Sigma_i|I_i(hkl) - \langle I(hkl)\rangle|/\Sigma_{hkl}\Sigma_i\, I_i(hkl)$.
[b] Numbers in parenthesis were calculated from data of the highest resolution shell.
[c] $R_{cryst} = \Sigma|\,|F_{obs}|-|F_{calc}|\,|/\Sigma|F_{obs}|$ where F_{calc} and F_{obs} are the calculated and observed structure factor amplitudes, respectively.
[d] R_{free} = as for R_{cryst}, but for ~5% of the total reflections chosen at random and omitted from refinement.
[e] Calculated using MolProbity [24].

2.5. Gel-filtration chromatography of the YtqB protein

The oligomeric status of the YtqB protein was estimated by gel-filtration chromatography. A Superdex 200 10/300 gel-filtration column (GE Healthcare) was equilibrated with a running buffer of 20 mM Hepes (pH 7.4), 150 mM NaCl, and 5 mM βME. The YtqB protein or gel filtration standards (Bio-Rad) were injected into the column in a volume of 300 μl, and the running buffer was run through the column. Protein elution was monitored by measuring the absorbance at 280 nm.

3. Results and discussion

3.1. The overall structure of YtqB

The YtqB structure was determined by molecular replacement and refined to 1.9 Å resolution (Table 1). Two YtqB molecules (defined as chains A and B in structure coordinates) were located in the asymmetric unit. The two chains did not exhibit any significant structural differences and were superimposable with a root mean square deviation (RMSD) value of 0.35 Å (Fig. S1A). The YtqB structure contains 172 (residues 1–103, 115–143, and 152–191 of chain A) or 171 (residues 1–103, 116–142, and 151–191 of chain B) residues from the entire molecule (residues 1–194), with two linkers (the β4–α5 and β5–α6 loops) and the three C-terminal residues missing in the final model.

YtqB adopts a single domain structure that consists of a central seven-stranded β-sheet (β1–β7) sandwiched by two layers of α-helices (α1–α2–α3 and α4–α5–α6) (Fig. 1A and B). The seven β-strands are aligned in the order of β3–β2–β1–β4–β5–β7–β6, and

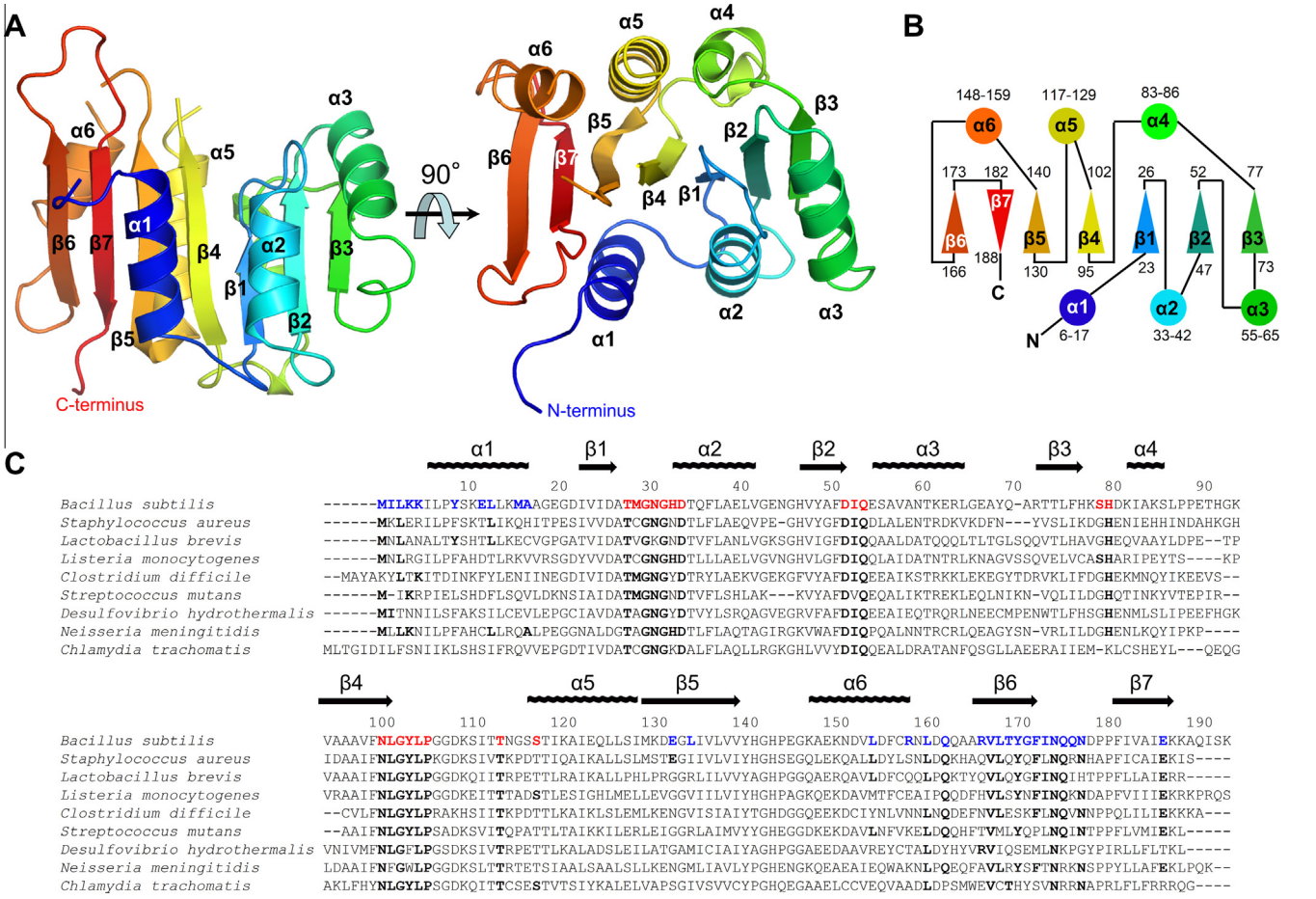

Fig. 1. The structure and sequence of YtqB. (A) The crystal structure of the YtqB monomer in a rainbow ribbon diagram from the N-terminus in blue to the C-terminus in red. (B) The secondary structure organization of YtqB. α-helices and β-strands are shown as circles and triangles, respectively, with numbers of boundary residues. (C) Sequence alignment of YtqB and its orthologs. In the YtqB sequence, the dimer interface residues and SAM-binding residues are colored in blue and red, respectively. The same types of residues in the sequences of the YtqB orthologs are bolded. (For interpretation of the references to color in this figure legend, the reader is referred to the web version of this article.)

only β7 runs anti-parallel to the other six parallel β-strands, indicating that YtqB possesses the canonical Rossmann-like fold of class I MTases [4,5]. Based on homologue searches in the Dali server, the YtqB structure exhibited the highest similarities to three unpublished structures of YtqB orthologs (PDB ID 3MTI from *Streptococcus thermophilus*, 3LBY from *Streptococcus mutans*, and 3EEY from *Clostridium thermocellum*) with RMSD values of 1.2–1.5 Å for 144–167 residues (Fig. S2A). The putative catalytic core structure of YtqB also resembles those of *E. coli* rRNA MTase RsmH (PDB ID 3TKA; RMSD, 2.2 Å for 163 residues) and rat catechol O-MTase (PDB ID 3OZR; RMSD, 2.4 Å for 158 residues) (Figs. S2B and S2C) [18,19].

3.2. Dimeric assembly of YtqB

Class I MTases have been reported to adopt various oligomeric forms, such as monomers, dimers, and tetramers, in solution. To determine the oligomeric status of YtqB, we carried out gel-filtration chromatography using the purified YtqB protein. YtqB (MW, 21.8 kDa) had an elution volume (16.3 ml) identical to that of a 44 kDa standard protein, indicating that YtqB is dimeric in solution (Fig. 2A). Consistently, the dimeric organization is preserved in the crystal lattice, which provides structural details about the dimeric architecture. In the homodimeric structure, the β-sheet of one YtqB molecule is continuously connected with that of the dimerization partner in an antiparallel manner by a non-crystallographic twofold symmetry axis that is located between β6 and β6′ (the prime denotes chain B) (Fig. 2B). The dimer interface buries a large accessible surface area (~1530 Å^2) on each side and is mainly located at the N-terminal region (α1) and the C-terminal region (β6, the α6–β6 loop, and the β6–β7 loop) (Figs. 1C and 2B). The dimer interface is centered by six β6–β6′ main-chain hydrogen bonds and the hydrophobic side-chain interactions of fourteen residues (Y9, L13, V168, L169, Y171, F173, and I174 in chain A, and their equivalent residues in chain B) (Fig. 2C). The extensive hydrophobic interactions in the center suggest that YtqB would be unstable as a monomer in aqueous solution. The hydrophobic center is surrounded by generally hydrophilic interactions, which would occlude water molecules from the hydrophobic region of the interface and function as an O-ring [20]. YtqB orthologs are likely to adopt the dimeric organization of YtqB for two reasons. First, the hydrophobic residues in the center of the interface and some of hydrophilic residues at the periphery are highly conserved among YtqB orthologs (Fig. 1C). Second, our YtqB structure and its ortholog structures exhibit the identical dimeric organization either by crystallographic or non-crystallographic two-fold symmetry (Fig. S2A).

3.3. YtqB binding to SAM

To provide structural details regarding the binding of YtqB to SAM, which is required for MTase activity, we have also determined the crystal structure of YtqB in complex with SAM (YtqB^{SAM})

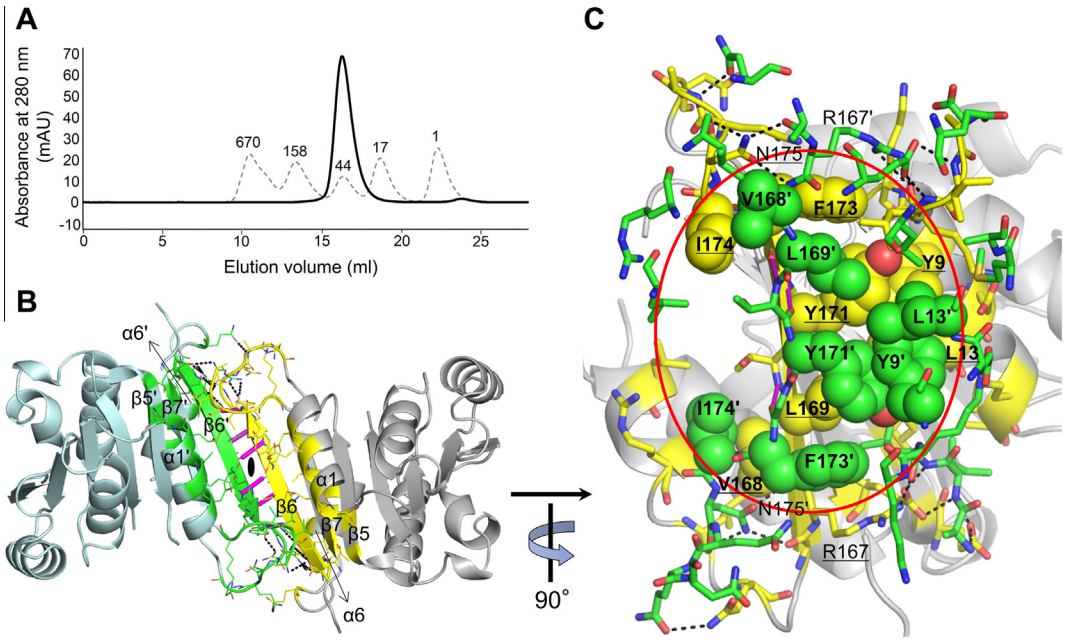

Fig. 2. Dimeric assembly of YtqB. (A) Gel-filtration chromatography of YtqB (a continuous line) and standard proteins (dashed lines; their molecular weights in kDa are shown above each peak). (B) The overall structure of the YtqB dimer. YtqB residues at the dimer interface are highlighted in yellow (chain A) and green (chain B) in the ribbon diagram of the YtqB dimer (chain A, gray; chain B, light blue) and are also shown in lines (carbon atoms of chain A, yellow; carbon atoms of chain B, green; oxygen atoms, red; nitrogen atoms, blue). Main-chain hydrogen bonds are represented by thick magenta lines and the other types of hydrogen bonds are shown in black dotted lines. (C) The YtqB dimer interface viewed from the left of the image shown in (B). The side chains of hydrophobic residues in the center of the dimer interface are shown as spheres (carbon atoms of chain A, yellow; carbon atoms of chain B, green; oxygen atoms, red), and enclosed by a red circle. For clarity, the ribbons of chain B were omitted. (For interpretation of the references to color in this figure legend, the reader is referred to the web version of this article.)

at 2.2 Å resolution (Fig. 3). Each YtqB molecule provides one SAM binding site and two SAM molecules of the YtqB^{SAM} dimer are distantly located (>40 Å) (Fig. 3A). SAM binding did not significantly alter the structure of the YtqB protein (RMSD values, 0.39–0.60 Å; Fig. S1) with the exception of the β4–α5 and β5–α6 loops, which were built in chain A only (residues 104–109 and 112–114 of the β4–α5 loop; residues 146–151 of the β5–α6 loop). The β4–α5 loop (residues 103–106 and 114) partially covers the top of SAM in chain A (Figs. 3C and S3). However, the role of the β4–α5 loop in SAM binding does not appear to be significant, given that the β4–α5 loop contacts SAM via the main chain through non-specific van der Waals interactions. As a result, the β4–α5 loop is not completely secured by SAM and still flexible with high B-factors (74 Å^2 for residues 104–115 of the loop over 56 Å^2 for the entire chain A). Moreover, the β4–α5 loop was disordered in chain B, and its interaction with the top of SAM was not observed.

Primary YtqB–SAM interactions are observed between the bottom and flanks of SAM and four loops of YtqB (the β1–α2, β2–α3, β3–α4, and β4–α5 loops) in both chains A and B (Figs. 1C, 3B, and 3C). The methionyl moiety of SAM is surrounded by six residues from the β1–α2 loop and two N-terminal residues of the β4–α5 loop. The adenosyl moiety primarily contacts the β2–α3 and β3–α4 loops. Both ends (the 3-amino-3-carboxypropyl group and the adenyl group) of SAM fit into slightly indented cavities of YtqB (Fig. 3B). The central part of SAM, which includes the S_δ atom and reactive C_ε methyl group, resides on the convex surface, allowing the C_ε methyl group to be exposed for the methyl transfer. The YtqB–SAM interaction is mostly hydrophilic with eleven hydrogen bonds (Figs. 3C and S3). As observed in other MTase-SAM complexes, the GxG motif (residues 30–32) of the β1–α2 loop makes contacts with the 3-amino-3-carboxypropyl group of SAM, and an acidic residue (D52) at the end of β2 forms two hydrogen bonds with the ribosyl moiety. In addition to the conserved contacts, the YtqB^{SAM} structure revealed numerous interactions specific to YtqB–SAM binding, including eight hydrogen bonds between the 3-amino-3-carboxypropyl group and four residues (T28, N31, H33, and D34) of the β1–α2 loop and α2 as well as between the adenyl group and two residues (S79 and H80) of the β3–α4 loop. The YtqB residues involved in SAM binding are highly conserved in YtqB orthologs, suggesting that YtqB orthologs would also use a similar SAM binding mechanism (Fig. 1C).

3.4. Implication of the YtqB structure in its substrate binding

YtqB has been annotated as an rRNA MTase in the database and shares structural similarity with the MTase domain of the *E. coli* rRNA MTase RsmH, implying that YtqB might methylate rRNA molecules (Fig. S2B) [18]. Consistently, electrostatic surface potential analysis revealed that the YtqB structure displays a positive patch (K4, K5, K11, K15, and R167) that would accommodate the phosphate backbone of RNA (Fig. S4A). However, YtqB residues that constitute the positive patch are not well conserved in YtqB orthologs (Fig. S4B). Moreover, YtqB lacks additional domains that are employed to specifically interact with a large RNA substrate, as shown for *E. coli* RumA and TrmA RNA MTases [10,21]. Thus, YtqB does not appear to be a stand-alone RNA MTase and might require a partner protein to recruit RNA molecules.

Another potential substrate of YtqB would be a small chemical that engages a smaller number of protein residues in binding compared to a large RNA molecule. Thus, a small chemical is often targeted by short class I MTases, as in the case of the 197-residue long TehB, which methylates the oxyanion derivatives of tellurium or selenium [22]. YtqB is also one of the shortest class I MTases, with 194 residues, and exhibits structural similarity with catechol O-MTase, which catalyzes the methyl transfer to small neurotransmitter chemicals such as dopamine and epinephrine (Fig. S2C) [19]. These findings support the notion that YtqB might methylate a small chemical.

Because YtqB does not possess the N-terminal extension or additional domains generally involved in substrate binding, it is

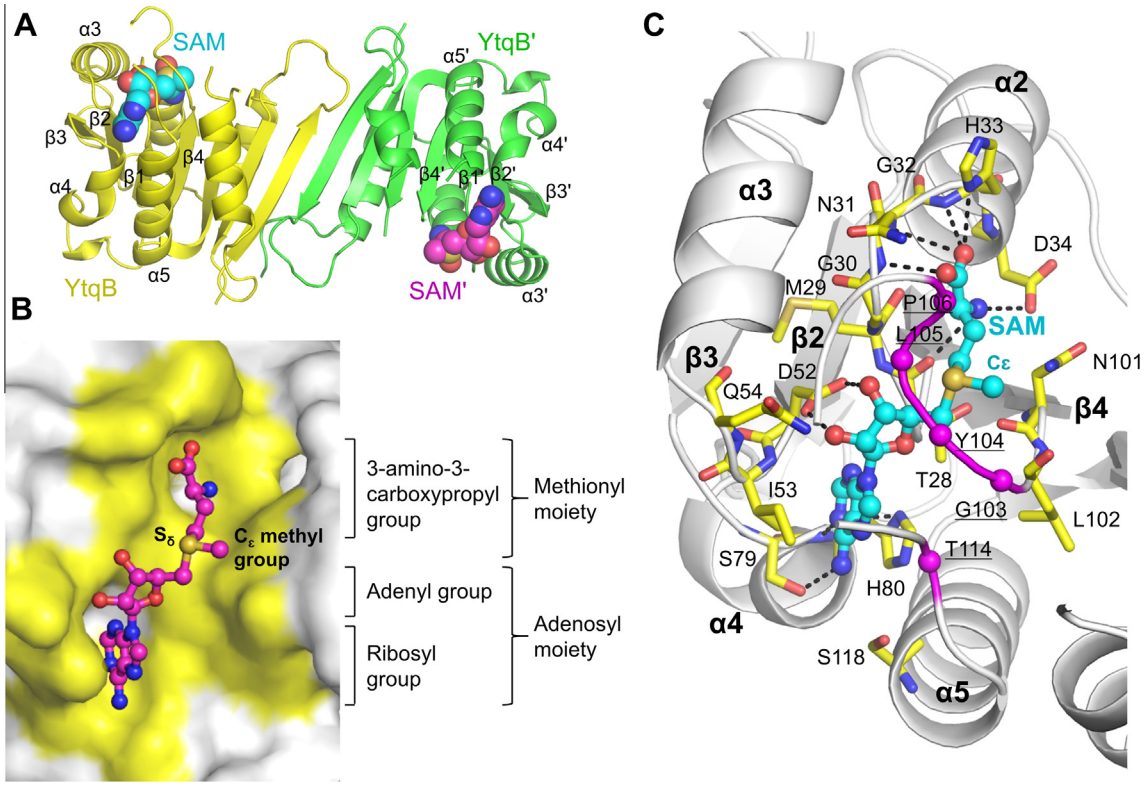

Fig. 3. YtqB binding to SAM. (A) The overall structure of the YtqB^{SAM} dimer viewed from the backside of the image shown in Fig. 2B. Each YtqB molecule in the dimer (chain A, yellow ribbons; chain B, green ribbons) is bound to one SAM molecule (spheres). (B) The SAM-binding pocket (yellow surface) of YtqB (chain B) and a SAM molecule (a ball-and-stick model; carbon, magenta; sulfur, gold; nitrogen, blue; oxygen, red). (C) A detailed view of the YtqB–SAM interaction. SAM is shown in a ball-and-stick model (carbon, cyan; oxygen, red; nitrogen, blue; gold, sulfur). SAM-contacting residues shared by both chains A and B are depicted as sticks (carbon, yellow; oxygen, red; nitrogen, blue). SAM-binding residues that are found only in chain A and not in chain B are traced in magenta and their Cα carbons are shown as magenta spheres. Hydrogen bonds are represented by black dotted lines. (For interpretation of the references to color in this figure legend, the reader is referred to the web version of this article.)

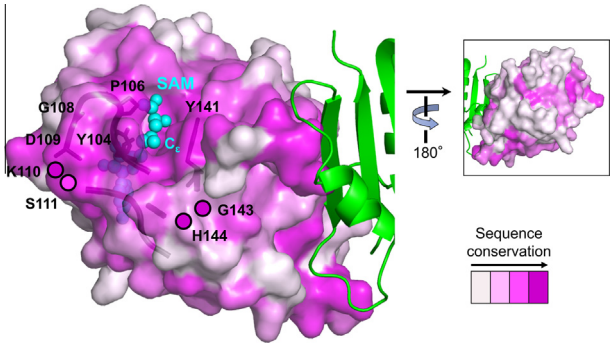

Fig. 4. Conserved β4–α5 and β5–α6 loops as a potential substrate binding site. YtqB chains A and B are shown in a transparent surface representation and green ribbons, respectively. SAM is depicted in cyan spheres. Sequence conservation was calculated using the ConSurf server [23] based on the sequence alignment shown in Fig. 1C and was color-coded in proportion to the intensity of the magenta color. Residues of the β4–α5 and β5–α6 loops (thick coils) conserved in at least six of nine species (Fig. 1C) are shown as sticks. Residues missing in the structure are represented by circles and color-coded by sequence conservation. High sequence conservation can be observed at and near the SAM binding site, and at the dimerization interface. In contrast, the backside shown in the small rectangle is poorly conserved. (For interpretation of the references to color in this figure legend, the reader is referred to the web version of this article.)

unclear how YtqB recruits a substrate for methylation. Interestingly, the β4–α5 loop of YtqB near the SAM cofactor is exceptionally long compared to other types of class I MTases, with 14 residues. The β4–α5 loop contacts SAM using its N-terminal region and further extends into solution as a highly flexible region without any noticeable contribution to protein core formation or SAM binding (Fig. 3C). The extension of the β4–α5 loop and its adjacent β5–α6 loop exhibit a high level of sequence similarity with YtqB orthologs (Figs. 1C and 4), suggesting their critical role. Thus, we propose that the β4–α5 or β5–α6 loops may interact with a substrate molecule and direct it toward the reactive methyl group of SAM.

In conclusion, our structural studies reveal that YtqB adopts the αβα sandwich architecture in a dimeric assembly. Each monomer binds one SAM molecule and exposes the reactive methyl group of SAM, potentially toward a methyl acceptor. Although our structural analysis provides clues to YtqB-substrate interactions, future studies are required to define the methylation mechanism.

Acknowledgments

X-ray diffraction datasets were collected at beamline 7A of the Pohang Accelerator Laboratory (Korea). This study was supported by Basic Science Research Program through the National Research Foundation of Korea (NRF) funded by the Ministry of Science, ICT & Future Planning (2012R1A1A1003701 to SIY) and by 2012 Research Grant from Kangwon National University (to SIY).

Appendix A. Supplementary data

Supplementary data associated with this article can be found, in the online version, at http://dx.doi.org/10.1016/j.bbrc.2014.03.026.

References

[1] A.W. Struck, M.L. Thompson, L.S. Wong, J. Micklefield, S-adenosyl-methionine-dependent methyltransferases: highly versatile enzymes in biocatalysis, biosynthesis and other biotechnological applications, ChemBioChem 13 (2012) 2642–2655.

[2] D.K. Liscombe, G.V. Louie, J.P. Noel, Architectures, mechanisms and molecular evolution of natural product methyltransferases, Nat. Prod. Rep. 29 (2012) 1238–1250.

[3] Y. Motorin, M. Helm, RNA nucleotide methylation, Wiley Interdiscip. Rev. RNA 2 (2011) 611–631.

[4] H.L. Schubert, R.M. Blumenthal, X. Cheng, Many paths to methyltransfer: a chronicle of convergence, Trends Biochem. Sci. 28 (2003) 329–335.

[5] R. Gana, S. Rao, H. Huang, C. Wu, S. Vasudevan, Structural and functional studies of S-adenosyl-L-methionine binding proteins: a ligand-centric approach, BMC Struct. Biol. 13 (2013) 6.

[6] D.J. Miller, N. Ouellette, E. Evdokimova, A. Savchenko, A. Edwards, W.F. Anderson, Crystal complexes of a predicted S-adenosylmethionine-dependent methyltransferase reveal a typical AdoMet binding domain and a substrate recognition domain, Protein Sci. 12 (2003) 1432–1442.

[7] A. Guelorget, M. Roovers, V. Guerineau, C. Barbey, X. Li, B. Golinelli-Pimpaneau, Insights into the hyperthermostability and unusual region-specificity of archaeal Pyrococcus abyssi tRNA m1A57/58 methyltransferase, Nucleic Acids Res. 38 (2010) 6206–6218.

[8] C. Zubieta, J.R. Ross, P. Koscheski, Y. Yang, E. Pichersky, J.P. Noel, Structural basis for substrate recognition in the salicylic acid carboxyl methyltransferase family, Plant Cell 15 (2003) 1704–1716.

[9] Y. Peng, D. Sartini, V. Pozzi, D. Wilk, M. Emanuelli, V.C. Yee, Structural basis of substrate recognition in human nicotinamide N-methyltransferase, Biochemistry 50 (2011) 7800–7808.

[10] T.T. Lee, S. Agarwalla, R.M. Stroud, A unique RNA Fold in the RumA-RNA-cofactor ternary complex contributes to substrate selectivity and enzymatic function, Cell 120 (2005) 599–611.

[11] A. Kumar, K. Saigal, K. Malhotra, K.M. Sinha, B. Taneja, Structural and functional characterization of Rv2966c protein reveals an RsmD-like methyltransferase from Mycobacterium tuberculosis and the role of its N-terminal domain in target recognition, J. Biol. Chem. 286 (2011) 19652–19661.

[12] W.S. Song, M. Hong, S.I. Yoon, Purification, crystallization and X-ray crystallographic studies on flagellin from Pseudomonas aeruginosa, Acta Crystallogr. Sect. F Struct. Biol. Cryst. Commun. 70 (2014) 200–202.

[13] W.S. Song, S.I. Yoon, Crystal structure of FliC flagellin from Pseudomonas aeruginosa and its implication in TLR5 binding and formation of the flagellar filament, Biochem. Biophys. Res. Commun. 444 (2014) 109–115.

[14] Z. Otwinowski, W. Minor, Processing x-ray diffraction data collected in oscillation mode, Methods Enzymol. 276 (1997) 307–326.

[15] A.J. McCoy, R.W. Grosse-Kunstleve, P.D. Adams, M.D. Winn, L.C. Storoni, R.J. Read, Phaser crystallographic software, J. Appl. Crystallogr. 40 (2007) 658–674.

[16] P. Emsley, K. Cowtan, Coot: model-building tools for molecular graphics, Acta Crystallogr. D Biol. Crystallogr. 60 (2004) 2126–2132.

[17] G.N. Murshudov, A.A. Vagin, E.J. Dodson, Refinement of macromolecular structures by the maximum-likelihood method, Acta Crystallogr. D Biol. Crystallogr. 53 (1997) 240–255.

[18] Y. Wei, H. Zhang, Z.Q. Gao, W.J. Wang, E.V. Shtykova, J.H. Xu, Q.S. Liu, Y.H. Dong, Crystal and solution structures of methyltransferase RsmH provide basis for methylation of C1402 in 16S rRNA, J. Struct. Biol. 179 (2012) 29–40.

[19] M. Ellermann, R. Paulini, R. Jakob-Roetne, C. Lerner, E. Borroni, D. Roth, A. Ehler, W.B. Schweizer, D. Schlatter, M.G. Rudolph, F. Diederich, Molecular recognition at the active site of catechol-O-methyltransferase (COMT): adenine replacements in bisubstrate inhibitors, Chemistry 17 (2011) 6369–6381.

[20] A.A. Bogan, K.S. Thorn, Anatomy of hot spots in protein interfaces, J. Mol. Biol. 280 (1998) 1–9.

[21] A. Alian, T.T. Lee, S.L. Griner, R.M. Stroud, J. Finer-Moore, Structure of a TrmA-RNA complex: a consensus RNA fold contributes to substrate selectivity and catalysis in m5U methyltransferases, Proc. Natl. Acad. Sci. USA 105 (2008) 6876–6881.

[22] H.G. Choudhury, A.D. Cameron, S. Iwata, K. Beis, Structure and mechanism of the chalcogen-detoxifying protein TehB from Escherichia coli, Biochem. J. 435 (2011) 85–91.

[23] A. Armon, D. Graur, N. Ben-Tal, ConSurf: an algorithmic tool for the identification of functional regions in proteins by surface mapping of phylogenetic information, J. Mol. Biol. 307 (2001) 447–463.

[24] V.B. Chen, W.B. Arendall 3rd, J.J. Headd, D.A. Keedy, R.M. Immormino, G.J. Kapral, L.W. Murray, J.S. Richardson, D.C. Richardson, MolProbity: all-atom structure validation for macromolecular crystallography, Acta Crystallogr. D Biol. Crystallogr. 66 (2010) 12–21.